JACS
JOURNAL OF THE AMERICAN CHEMICAL SOCIETY

Article

pubs.acs.org/JACS

Molecular Precision and Enzymatic Degradation: From Readily to Undegradable Polymeric Micelles by Minor Structural Changes

Merav Segal,[†,‡] Ram Avinery,[‡,§] Marina Buzhor,[†,‡] Rona Shaharabani,[‡,∥] Assaf J. Harnoy,[†,‡] Einat Tirosh,[‡,∥] Roy Beck,[‡,§] and Roey J. Amir*[,†,‡]

[†]Department of Organic Chemistry, School of Chemistry, Faculty of Exact Sciences, Tel-Aviv University, Tel-Aviv 6997801, Israel
[‡]Tel-Aviv University Center for Nanoscience and Nanotechnology, Tel-Aviv University, Tel-Aviv 6997801, Israel
[§]School of Physics and Astronomy, Faculty of Exact Sciences, Tel-Aviv University, Tel-Aviv 6997801, Israel
[∥]Department of Physical Chemistry, School of Chemistry, Faculty of Exact Sciences, Tel-Aviv University, Tel-Aviv 6997801, Israel

Supporting Information

ABSTRACT: Studying the enzymatic degradation of synthetic polymers is crucial for the design of suitable materials for biomedical applications ranging from advanced drug delivery systems to tissue engineering. One of the key parameters that governs enzymatic activity is the limited accessibility of the enzyme to its substrates that may be collapsed inside hydrophobic domains. PEG-dendron amphiphiles can serve as powerful tools for the study of enzymatic hydrolysis of polymeric amphiphiles due to the monodispersity and symmetry of the hydrophobic dendritic block, which significantly simplifies kinetic analyses. Using these hybrids, we demonstrate how precise, minor changes in the hydrophobic block are manifested into tremendous changes in the stability of the assembled micelles toward enzymatic degradation. The obtained results emphasize the extreme sensitivity of self-assembly and its great importance in regulating the accessibility of enzymes to their substrates. Furthermore, the demonstration that the structural differences between readily degradable and undegradable micelles are rather minor, points to the critical roles that self-assembly and polydispersity play in designing biodegradable materials.

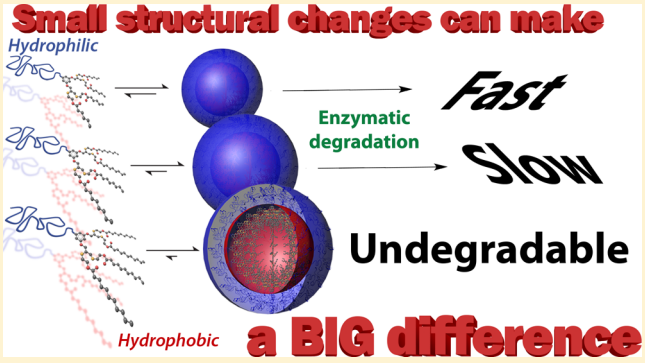

INTRODUCTION

Studying the enzymatic degradation of synthetic polymers is crucial for the design of biodegradable materials for applications ranging from polymeric coatings of medical devices[1,2] to tissue engineering[3,4] preparation of edible coatings,[5,6] cosmetics,[7,8] and drug formulations.[9−11] In the field of controlled drug delivery, the overexpression of disease-associated enzymes can potentially be utilized for the selective release of active drug molecules only at the desired disease site.[12,13] Several polymeric architectures, including linear block copolymers,[14−18] peptide containing copolymers,[19] dendrimers,[20−22] hyperbranched polymers,[23,24] and linear-dendron copolymers,[25] have been explored as building blocks for the construction of enzyme-responsive micelles and other smart assemblies.[26−28] Regardless of the polymeric architecture, a key parameter that governs the enzymatic activity is the accessibility of the enzyme to its substrates that may be buried inside hydrophobic domains or cores in the case of micellar assemblies.[29−32] Recently, we used PEG-dendron amphiphiles to study enzymatic hydrolysis of polymeric amphiphiles.[33−35] The inherent monodispersity and symmetry of the hydrophobic dendritic block of PEG-dendron hybrids, which were introduced in a pioneering work by Fréchet, Gitsov, Wooley, and Hawker in the early 1990s,[36,37] enabled us to carry out a detailed kinetic analysis of their enzymatic degradation. The observed correlation between higher critical micelle concentration (CMC) values and faster disassembly rates for hybrids with longer PEGs indicated that the enzyme could not reach the hydrophobic core of the micelle and the cleavable end-groups must be on the surface or outside of the micelle for the cleavage to occur.[33,35] These conclusions were in good agreement with the results of enzymatic hydrolysis of other polymeric systems in the literature.[29,30]

Motivated by the high molecular resolution that was obtained in the previous studies, we decided to utilize the structural precision of linear-dendritic based amphiphilic hybrids in order to examine how minor changes in the length of the hydrophobic dendritic end-groups affect the self-assembly and enzymatic degradation of the formed polymeric micelles. Aliphatic esters were selected as enzymatically cleavable end-groups due to the commercial availability of aliphatic carboxylic acid precursors with chains of different lengths. Three carboxylic acids were chosen for the

Received: October 13, 2016
Published: December 19, 2016

DOI: 10.1021/jacs.6b10624
J. Am. Chem. Soc. 2017, 139, 803−810

introduction of the enzymatically cleavable end-groups: hexanoic acid (Hex), nonanoic acid (Non), and undecanoic acid (Und; Figure 1 and Scheme 1). Porcine liver esterase (PLE) was selected as the activating enzyme.

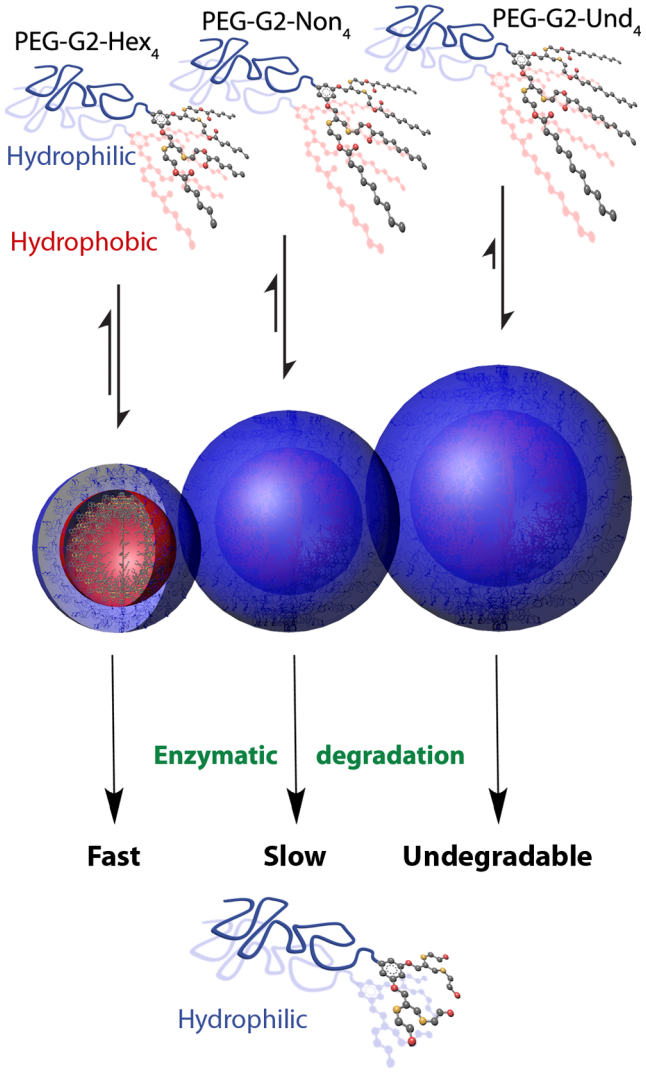

Figure 1. Schematic representation of the molecular architecture of second-generation PEG-dendron amphiphilic hybrids with four aliphatic alkyl chains of increasing length (PEG-G2-Hex$_4$, PEG-G2-Non$_4$, and PEG-G2-Und$_4$) as enzymatically cleavable end-groups, and the hydrophilic degradation product.

RESULTS AND DISCUSSION

The synthesis followed a high yielding accelerated approach for the preparation of the hybrids as illustrated in Scheme 1. A 5 kDa PEG amine, **1**, was conjugated to diacetylene containing branching unit **2**, through an amide bond to give hybrid **3**, followed by thiol−yne reaction[38,39] with 2-mercaptoethanol to yield hybrid **4**.[34] Esterification reactions with excess of hexanoic, nonanoic, and undecanoic acids were carried out using DCC and DMAP (Steglich esterification)[40] to yield the final hybrids: PEG-G2-Hex$_4$, PEG-G2-Non$_4$, and PEG-G2-Und$_4$, respectively, in excellent overall yields. The final hybrids were characterized by ^{1}H NMR, ^{13}C NMR, GPC, MALDI-TOF MS, IR, UV absorbance, and HPLC, and the experimental data

Scheme 1. Synthesis of PEG-G2-Dendron Hybrids

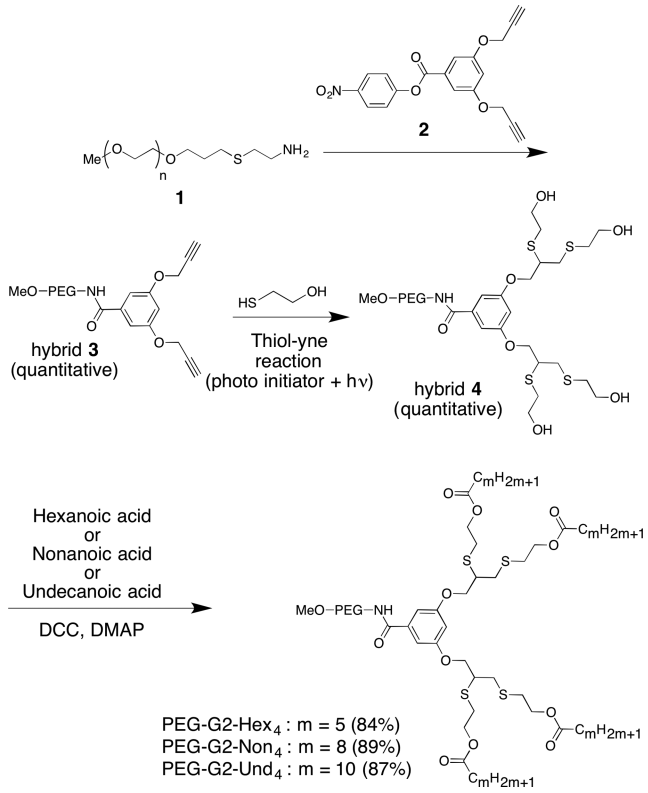

were in excellent agreement with the expected results (see Table 1 and SI).

The CMC values of the amphiphiles were expected to decrease with increasing the length of the alkyl-based end-group due to the increase in the hydrophobicity of the dendritic block. CMCs were measured using Nile red as a solvatochromic fluorescent probe.[41] There was a slight decrease in CMC value as the length of the alkyl end-group increased (Table 1). After the CMC values were determined, we characterized the assembled structures by dynamic light scattering (DLS); diameters of 16, 23, and 31 nm were measured for PEG-G2-Hex$_4$, PEG-G2-Non$_4$, and PEG-G2-Und$_4$, respectively (Table 1 and Figure 2a). Transmission electron microscopy (TEM) images also confirmed the assembly into nanosize spherical objects with similar diameters (Figure 2b−d). ^{1}H NMR spectra of the hybrids in D_2O gave further support for the formation of core−shell micelles as only the PEG protons were observed in the spectra, due to the decreased mobility and short relaxation times of the hydrophobic protons (see SI).[42]

Although all three amphiphilic hybrids self-assembled into spherical micelles, the diameters of the micelles increased significantly more than expected based on the differences in lengths of the hydrophobic end-groups. If one considers the structural changes in the end-groups of the three hybrids, the elongation of the end-groups should lead to a change of no more than 2−4 Å in the diameter of the micelles; however, the DLS results clearly showed a difference in diameter of more than 6 nm, which is an order of magnitude larger than the expected difference. To confirm the increase in diameters and to estimate the aggregation numbers of the three hybrids, which could help to explain the different sizes, we used small-angle X-ray scattering (SAXS) technique.[43] We were encouraged to see that the radii of gyration (R_g) from SAXS analyses (Table 1)

DOI: 10.1021/jacs.6b10624
J. Am. Chem. Soc. 2017, 139, 803−810

Table 1. Molecular Properties of the PEG-G2-Dendron Hybrids and Their Micellar Assemblies

Hybrid	Mn[a] (kDa)	PDI[a]	Mp[b] (kDa)	Calculated Mn[c] (kDa)	PEG:Dendron weight ratio[c]	CMC[d] (μM) (mg/L)	R_H[e] (nm)	R_g[f] (nm)	Aggregation number[f]
PEG-G2-Hex$_4$	5.6	1.03	6.1	6.035	83:17	4 ± 1	8 ± 3	7.4 ± 0.6	32 ± 3
						(24 ± 6)			
PEG-G2-Non$_4$	5.6	1.04	6.2	6.204	81:19	3 ± 1	12 ± 4	8.5 ± 1.0	51 ± 1
						(19 ± 6)			
PEG-G2-Und$_4$	5.7	1.03	6.4	6.316	79:21	2 ± 1	16 ± 7	11.0 ± 0.6	90 ± 5
						(13 ± 6)			

[a]Measured by GPC using PEG standards. [b]Measured by MALDI-TOF MS. [c]Calculated based on PEG 5 kDa and the expected exact mass of the dendrons. [d]Determined using Nile red. [e]Hydrodynamic radius measured by DLS. [f]Radius of gyration and aggregation numbers as measured by SAXS.

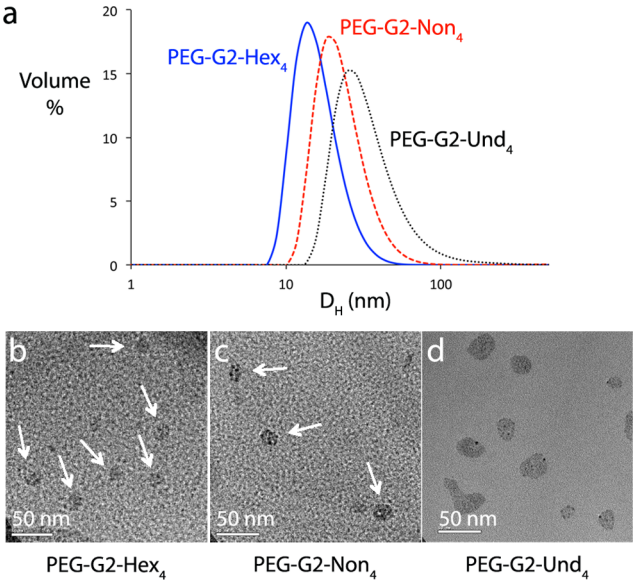

Figure 2. (a) Sizes of the micelles determined by DLS. (b-d) TEM images for (b) PEG-G2-Hex$_4$, (c) PEG-G2-Non$_4$, and (d) PEG-G2-Und$_4$.

were in good correlation with the DLS data (for spheres R_g = 0.775 R_H). The SAXS results also showed that the relatively small changes in the length of the hydrophobic end-groups led to a nonproportional increase in the aggregation numbers of the micelles, ranging from around 30 for the PEG-G2-Hex$_4$ to 50 for PEG-G2-Non$_4$ to 90 for PEG-G2-Und$_4$ (Table 1). The increased packing of polymeric hybrids with longer hydrophobic chains likely explains the unexpectedly large sizes of the micelles formed by PEG-G2-Non$_4$ and PEG-G2-Und$_4$, which were observed by DLS, TEM, and SAXS. It is interesting to note that whereas the CMC values varied only slightly, the aggregation numbers were significantly more sensitive to the increase in hydrophobicity of the end-groups.

After we completed the characterization of the formed micelles, we studied their enzymatically induced disassembly. Assuming that the hybrids are most likely hydrolyzed by the enzyme when not associated with the micelles through an equilibrium-based mechanism,[33,35,44] we expected to see a direct correlation between the CMC values and enzymatic hydrolysis rates. As the hybrids with the longer alkyl chains have lower CMC values, they should have a lower degree of dissociation and hence there should be a lower concentration of non-micelle-associated monomeric hybrids available for enzymatic cleavage. On the other hand, hybrids with higher CMC values should be present in relatively higher concentrations in their monomeric form and hence should be more susceptible to enzymatic hydrolysis. To study the enzymatic hydrolysis and disassembly of the micelles we combined two characterization techniques: HPLC was used to directly monitor the enzymatic hydrolysis, and fluorescence spectroscopy of encapsulated Nile red was used to monitor the micelle disassembly. Samples of the polymeric micelles ([hybrid] = 25 μM) in PBS, pH 7.4 were incubated at 37 °C in the presence of the activating enzyme and were periodically monitored by HPLC to analyze the degree of enzymatic hydrolysis and the formation of the hydrophilic tetra-hydroxy hybrid **4**.

Based on the relatively small differences in the CMC values of the three amphiphilic hybrids, small variations in the enzymatic degradation and disassembly rates could be expected if the enzyme does not have a clear preference for one of the three types of hydrophobic chains. To our surprise, HPLC data indicated that PEG-G2-Hex$_4$ was completely degraded into hydrophilic hybrid **4** in the presence of 27 nM PLE in less than 30 min (Figure 3a,d), whereas PEG-G2-Non$_4$ and PEG-G2-Und$_4$ were not degraded to a significant extent after 17 h. A 5-fold increase in the concentration of the enzyme led to 35% degradation of hybrid PEG-G2-Non$_4$ (Figure 3e), but almost no hydrolysis of PEG-G2-Und$_4$, after 17 h at 37 °C. Only when we increased the concentration of the enzyme by another 10-fold to 1.35 μM, around 5 mol % of the concentration of the hybrid, did we achieve full enzymatic hydrolysis of the nonanoic-based esters (Figure 3b,f). It is highly interesting to note that even under this high concentration of the activating enzyme, only minor hydrolysis was observed for hybrid PEG-G2-Und$_4$ (Figure 3c,f).

Fluorescence measurements of polymeric solutions containing Nile red (1.25 μM) and the activating enzyme were further used to follow the enzymatically induced disassembly. To ensure that the encapsulation of the dye did not alter the stability of the micelles, we followed the enzymatic degradation in the presence and absence of Nile red and observed similar degradation rates by HPLC (see SI). As the Nile red molecules are released from the hydrophobic cores into the more hydrophilic aqueous environment their fluorescence emission decreases. Fluorescence spectra of encapsulated Nile red were measured in the presence of 2.7 nM PLE for PEG-G2-Hex$_4$ and 135 nM for PEG-G2-Non$_4$ (Figure 4). The observed decrease in the emission intensities due to disassembly of the micelles and release of Nile red showed good correlation with the

DOI: 10.1021/jacs.6b10624
J. Am. Chem. Soc. 2017, 139, 803−810

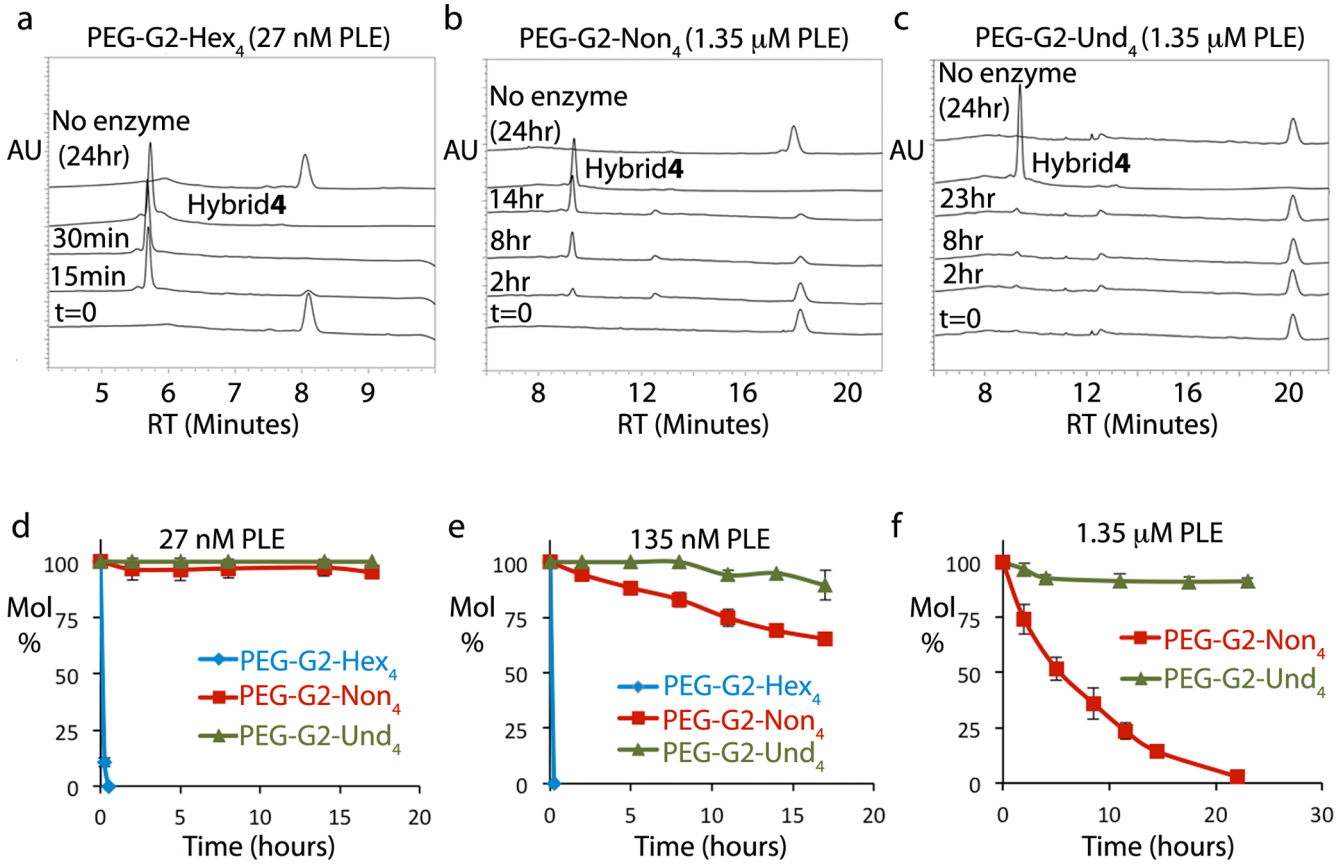

Figure 3. (a–c) HPLC traces and (d–f) plots of mol % as a function of time for the enzymatic degradation of hybrids PEG-G2-Hex_4, PEG-G2-Non_4, and PEG-G2-Und_4. All experiments were done with constant hybrid concentration (25 μM), and the concentrations of the enzyme PLE were varied as indicated.

hydrolysis rate of the amphiphilic hybrids, which were measured using HPLC.

Intrigued by the substantial differences in the stabilities of the three hybrids to enzymatic degradation and as both PEG-G2-Non_4 and PEG-G2-Und_4 did not show any crystallinity by differential scanning calorimetry (DSC), which could explain the tremendous range of micellar stabilities, we decided to test whether the observed kinetic trend was simply due to substrate specificity of the enzyme, which might prefer to cleave the shorter alkyl chain rather than the longer ones. To examine this hypothesis, we prepared zero-generation (G0) hybrids bearing only a single alkyl chain as their enzymatic substrate (Scheme 2).

The three G0 hybrids were synthesized by conjugating a 5 kDa PEG amine, **1**, to an activated ester of 4-(allyloxy)benzoic acid, **5**, followed by thiol–ene reaction with 2-mercaptoethanol to yield hybrid **7**.[35] Esterification reactions with excess of hexanoic, nonanoic, and undecanoic acids in the presence of DCC and DMAP yielded the final hybrids: PEG-G0-Hex, PEG-G0-Non, and PEG-G0-Und, respectively, in excellent overall yields (Scheme 2).

The decrease in the relative hydrophobicity of the G0 hybrids in comparison with the G2 hybrids led to higher CMC values: 55 ± 1 μM for PEG-G0-Hex, 41 ± 3 μM for PEG-G0-Non, and 16 ± 2 μM for PEG-G0-Und. To estimate the quality of each of the G0 hybrids to serve as a substrate for the activating esterase, we wished to eliminate the effect of self-assembly on the enzymatic reaction. Hence, the enzymatic degradation was studied at a hybrid concentration of 10 μM, which is below the CMC value that was measured for PEG-G0-Und. As the enzymatic hydrolysis of the G0 hybrids was much faster than that of the G2 hybrids, we decreased the concentration of the enzyme to 16 pM in order to slow down the reaction rates and allow the use of HPLC to monitor the enzymatic degradation.

We were fascinated to learn that at 10 μM, which is well below the CMC values of all G0 hybrids, the longer undecanoate ester was actually the best substrate, followed by the slightly shorter nonanoate ester, and the hexanoate ester was the slowest to be degraded (Figure 5a). When we measured the enzymatic degradation for these G0 hybrids at a concentration of 600 μM, which is well above their CMC, the kinetic trend differed: PEG-G0-Non was the first to be fully hydrolyzed, followed by PEG-G0-Und, with the PEG-G0-Hex again the slowest to be cleaved (Figure 5b). These results give a very interesting insight into the importance of self-assembly in the stabilization of micellar assemblies against enzymatic degradation of the assembled polymeric amphiphiles. Furthermore, it strengthens the hypothesis that if the enzyme could reach the hydrophobic core of the micelle, the undecanoate chains, which are the best substrates, should also be hydrolyzed more rapidly than the hexanoate and nonanoate chains when the hybrids are assembled.

Although the results of the enzymatic hydrolysis of the G0 based hybrids clearly indicated that the longer undecanoate chain is a good substrate for the activating enzyme, we could not disregard the possibility that steric hindrance, which results from the close proximity of two adjacent end-groups in the case

DOI: 10.1021/jacs.6b10624
J. Am. Chem. Soc. 2017, 139, 803–810

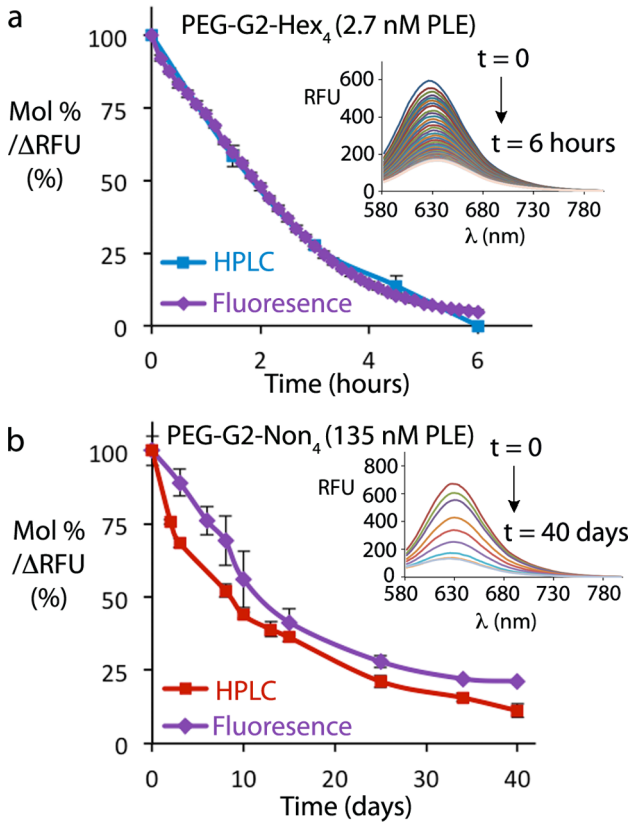

Figure 4. Overlays of HPLC and fluorescence data (insets: fluorescence spectra) for the enzymatic degradation of hybrids (a) PEG-G2-Hex$_4$ ([hybrid] = 25 μM, [enzyme] = 2.7 nM) and (b) PEG-G2-Non$_4$ ([hybrid] = 25 μM, [enzyme] = 135 nM).

Scheme 2. Synthesis of PEG-G0-Dendron Hybrids

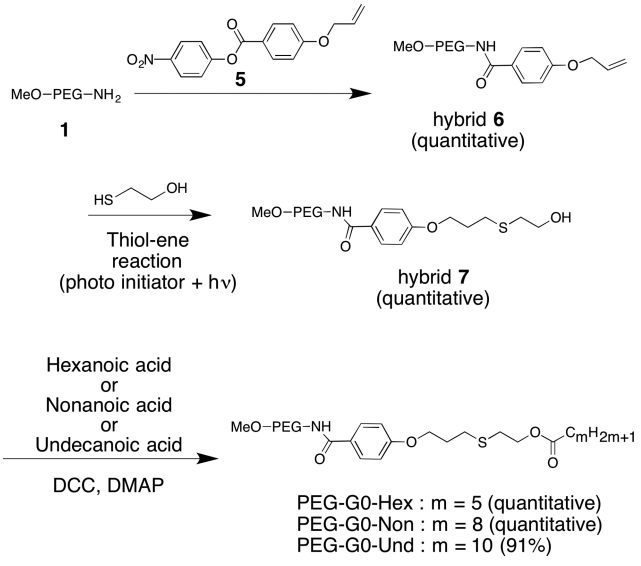

of the G2 based hybrids, limits access of the enzyme to the cleavable esters. To rule this out, we prepared first-generation (G1) hybrids bearing dendrons with only two alkyl end-groups (Scheme 3). The two alkyl esters were connected through the same thiol–yne approach that was used for synthesis of the G2 hybrids, but instead of the diacetylene branching unit, we used a monoacetylene one. This allowed us to place two adjacent end-groups in the exact same manner as in the case of the G2

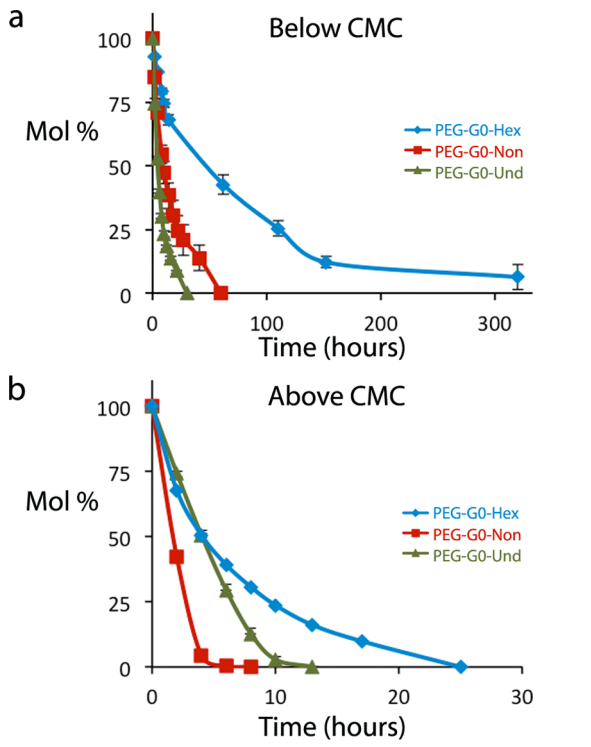

Figure 5. HPLC data for the enzymatic degradation of hybrids PEG-G0-Hex, PEG-G0-Non, and PEG-G0-Und (a) below ([hybrid] = 10 μM, [enzyme] = 16 pM) and (b) above ([hybrid] = 600 μM, [enzyme] = 160 pM) their CMCs.

Scheme 3. Synthesis of PEG-G1-Dendron Hybrids

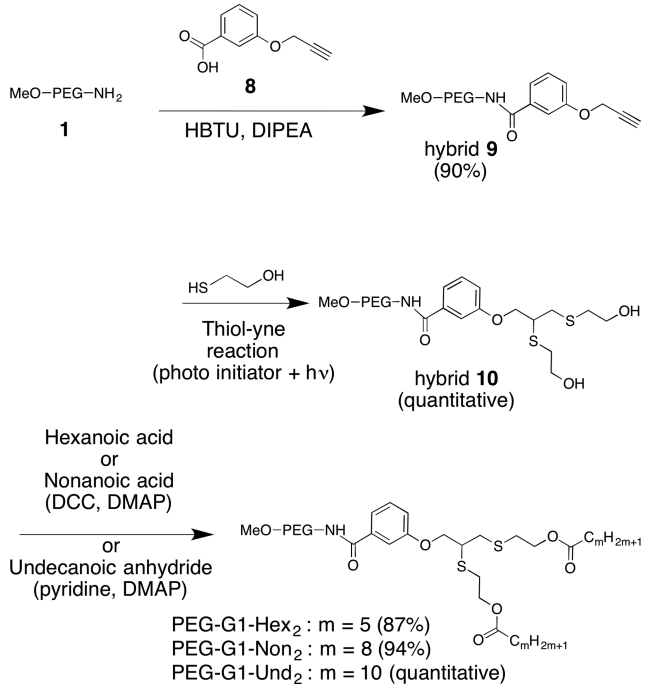

hybrids. The three G1 hybrids were synthesized by conjugating a 5 kDa PEG amine, **1**, to 3-(propargyloxy) benzoic acid, **8**,[45] in the presence of HBTU to give hybrid **9**. Thiol–yne reaction with 2-mercaptoethanol yielded hybrid **10**. Esterification reactions with excess hexanoic or nonanoic acids in the presence of DCC and DMAP or with undecanoic anhydride in

DOI: 10.1021/jacs.6b10624
J. Am. Chem. Soc. 2017, 139, 803–810

the presence of pyridine and DMAP yielded the final hybrids: PEG-G1-Hex$_2$, PEG-G1-Non$_2$, and PEG-G1-Und$_2$, respectively, in excellent overall yields (Scheme 3).

CMC measurements of the G1-dendron hybrids gave intermediate values between those obtained for the G0 and G2 hybrids: 12 ± 1 μM, 10 ± 1 μM, and 9 ± 2 μM for PEG-G1-Hex$_2$, PEG-G1-Non$_2$, and PEG-G1-Und$_2$, respectively. DLS confirmed the formation of micelles with diameters of 15−20 nm (see SI). The enzymatic degradation experiments were carried out by incubating the formed micelles ([hybrid] = 100 μM) with the activating enzyme (2.7 nM) and formation of the fully cleaved hybrid **10** was monitored by HPLC. The obtained data showed relatively fast degradation of the hexanoate- and nonanoate-containing hybrids. The undecanoate-containing hybrid PEG-G1-Und$_2$ was the slowest to be cleaved, but full cleavage was achieved after 3 days (Figure 6). These results demonstrate that the enzyme can indeed cleave the long alkyl chains even when two chains are in very close spatial proximity.

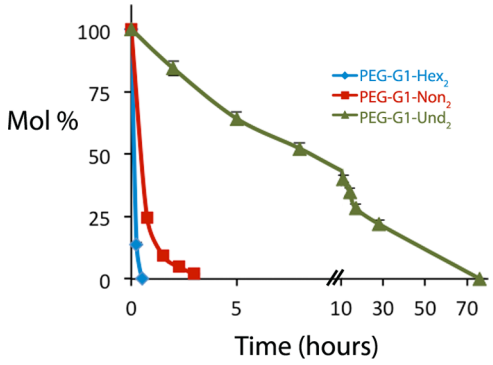

Figure 6. HPLC data for the enzymatic degradation of hybrids PEG-G1-Hex$_2$, PEG-G1-Non$_2$, and PEG-G1-Und$_2$ ([hybrid] = 100 μM, [enzyme] = 2.7 nM).

Overall, the obtained results for all nine G0-G2 based hybrids demonstrate the great sensitivity of micellar stability to small molecular changes in the hydrophobic block. To explore whether these drastic variations were merely a response to the change in amphiphilicity, we synthesized a G2-hybrid based on a 2 kDa PEG and four hexanoate chains with a hydrophobic weight fraction of 35%. Comparison of its degradation and disassembly rates with those of the 5 kDa based hybrid (PEG-G2-Hex$_4$), which has a hydrophobic weight fraction of 17%, showed the expected slower degradation and disassembly of the former by the enzyme (Figure 7). The differences were drastically smaller than the differences between PEG-G2-Hex$_4$ and PEG-G2-Non$_4$ or PEG-G2-Und$_4$, although the hydrophobic weight fractions of PEG-G2-Non$_4$ or PEG-G2-Und$_4$ are only 19% and 21%, respectively. These results clearly show that decreasing the hydrophilic block by a factor of 2.5 roughly doubled the degradation time. However, the minor changes in the length of the hydrophobic end-groups led to a more substantial increase in stability, although the overall amphiphilic ratio did not change significantly. These kinetic results illustrate the critical and tremendous role of the size of the hydrophobic block in determining its aggregation and consequent micellar stability, in addition to the milder contribution of the ratio between the hydrophilic and hydrophobic blocks.

To provide a further demonstration of the sensitivity of the degradation rates to minor changes in the hydrophobic block, we followed the degradation of mixtures of PEG-G2-Hex$_4$ and

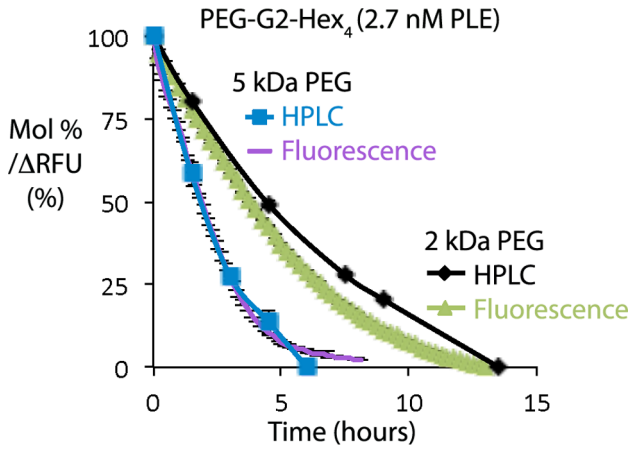

Figure 7. HPLC data and change in fluorescence with time for the enzymatic degradation of PEG-G2-Hex$_4$ hybrids composed of either a 2 kDa or a 5 kDa PEG chains (overall hybrids concentration ~25 μM, [enzyme] = 2.7 nM).

either PEG-G2-Non$_4$ or PEG-G2-Und$_4$ at different ratios (3:1, 1:1, and 1:3) by HPLC. The results, overlaid over the degradation profile of pure PEG-G2-Hex$_4$ are presented in Figure 8. It is clear that for both types of mixtures, no

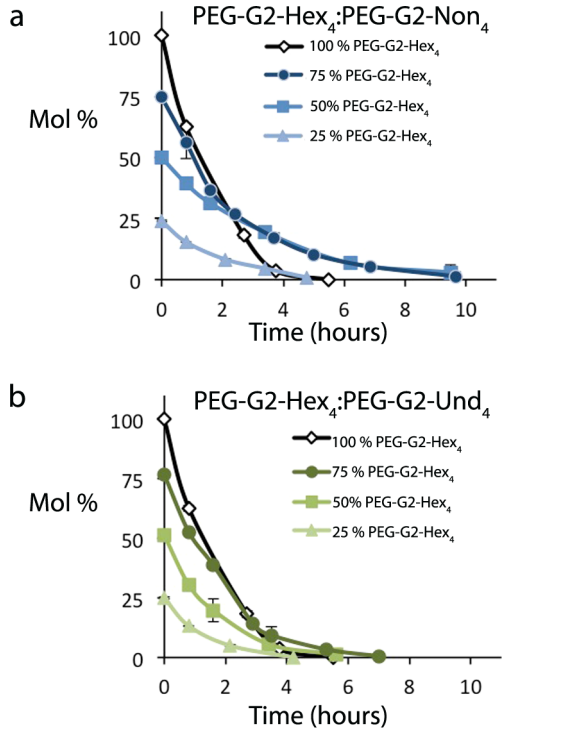

Figure 8. HPLC data for the enzymatic degradation of PEG-G2-Hex$_4$ hybrids in the presence of (a) PEG-G2-Non$_4$ and (b) PEG-G2-Und$_4$ at different ratios (overall hybrids concentration ~160 μM, [enzyme] = 27 nM).

hydrolysis was observed for the more hydrophobic hybrids PEG-G2-Non$_4$ or PEG-G2-Und$_4$ (see SI), whereas the PEG-G2-Hex$_4$ hybrids were completely degraded by the enzyme. It is interesting to point out that mixing the PEG-G2-Hex$_4$ with PEG-G2-Und$_4$ led to a minor decrease in the enzymatic degradation rate of the former. In its mixtures with PEG-G2-Non$_4$, the degradation rate of PEG-G2-Hex$_4$ was even slower.

DOI: 10.1021/jacs.6b10624
J. Am. Chem. Soc. 2017, 139, 803−810

These results indicate that the formation of mixed micelles can stabilize the less hydrophobic PEG-G2-Hex_4 hybrid.

It is important to consider that minimal structural alternations between the hybrids in each G0-G2 series resulted in huge differences in degradation rates, which ranged from minutes to undegradable assemblies. To further examine the sensitivity of the enzymatic hydrolysis to the structural changes, we prepared a mixture of mixed hybrids with different combinations of hexanoate and nonanoate based end-groups. The hybrids were synthesized by reacting hybrid **4** with 1:1 mixture of hexanoic and nonanoic acids. We expected to obtain a mixture of five hybrids bearing different ratios of hexanoate and nonanoate based end-groups: PEG-G2-Hex_4, PEG-G2-Hex_3Non_1, PEG-G2-Hex_2Non_2, PEG-G2-Hex_1Non_3, and PEG-G2-Non_4. HPLC chromatogram of the mixture indeed showed the formation of five peaks with two of the peaks overlapping with the peaks of pure PEG-G2-Hex_4 and PEG-G2-Non_4, which were synthesized earlier (Figure 9a). On the basis of the pattern of the obtained peaks, we correlated the new three peaks with the mixed hybrids: PEG-G2-Hex_3Non_1, PEG-G2-Hex_2Non_2, and PEG-G2-Hex_1Non_3. HPLC analysis of the enzymatic hydrolysis of the mixture gave a striking demonstration of the effect of minor structural changes on enzymatic degradation as the hybrids showed a clear decrease in their hydrolysis rate with increase in the number of nonanoate end-groups (Figure 9b). This extreme sensitivity of the stabilities of the hybrids toward enzymatic hydrolysis suggests that polydispersity of the hydrophobic block should be carefully considered in the design and development of materials with controllable degradation rates. The obtained results clearly show that polymers with slightly smaller hydrophobic blocks are more rapidly cleaved than those with larger ones, which may even be undegradable. This may explain the partial enzymatic degradation that is reported for many amphiphilic materials.[14] Nevertheless, the broad range of stabilities that was achieved here demonstrates the ability to design materials with adjustable degradation rates by simple minor structural alternations.

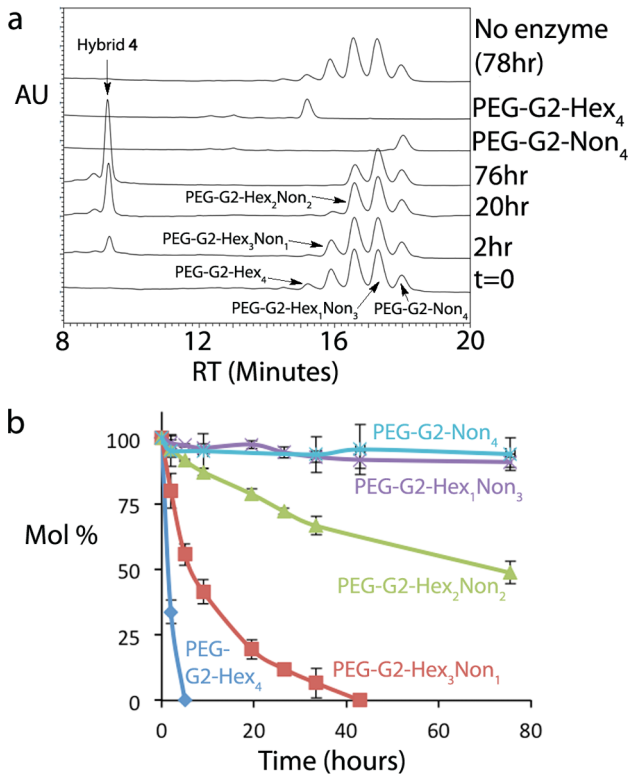

Figure 9. (a) HPLC traces and (b) changes in mol % vs time of mixed hybrids: PEG-G2-Hex_4, PEG-G2-Hex_3Non_1, PEG-G2-Hex_2Non_2, PEG-G2-Hex_1Non_3, and PEG-G2-Non_4 upon their enzymatic degradation (overall hybrids concentration ~160 μM, [enzyme] = 27 nM).

CONCLUSIONS

To summarize, we prepared ten amphiphilic PEG-dendron hybrids based on zero- to second-generation dendrons bearing one to four cleavable hydrophobic end-groups. The dendritic end-groups were selected from hexanoic acid, nonanoic acid, and undecanoic acid, which were conjugated to the dendron through enzymatically cleavable esters. The monodispersity of the dendrons allowed us to achieve extremely high molecular resolution in studying the effects of small changes in the dendron end-group on the size and stability of the self-assembled micelles. The results of our study demonstrate the key role of self-assembly in determining the accessibility and availability of degradable amphiphilic polymers to the activating enzyme. The extreme sensitivity of micellar stability to small changes of the molecular structure indicates that polydispersity may be a crucial factor for achieving greater control over the release rates of controlled drug delivery platforms and the degradation rates of biodegradable materials.

ASSOCIATED CONTENT

Supporting Information

The Supporting Information is available free of charge on the ACS Publications website at DOI: 10.1021/jacs.6b10624.

Detailed experimental information, characterization data, and control experiments (PDF)

AUTHOR INFORMATION

Corresponding Author

*amirroey@tau.ac.il

ORCID

Ram Avinery: 0000-0002-9580-4989

Roey J. Amir: 0000-0002-8502-3302

Notes

The authors declare no competing financial interest.

ACKNOWLEDGMENTS

This research was supported by the Israel Science Foundation (Grants No. 966/14 and 2221/14). R.B. acknowledges the support of Israel Science Foundation (Grant No. 550/15). We thank the staff of BioSAXS beamline at the P12 EMBL beamline at Hamburg, Germany. Travel grants to the synchrotron facility were provided by BioStruct-X.

REFERENCES

(1) Langer, R.; Tirrell, D. A. *Nature* **2004**, *428*, 487.
(2) Farah, S.; Anderson, D. G.; Langer, R. *Adv. Drug Delivery Rev.* **2016**, *107*, 367.
(3) Jia, X.; Kiick, K. L. *Macromol. Biosci.* **2009**, *9*, 140.
(4) Van Vlierberghe, S.; Dubruel, P.; Schacht, E. *Biomacromolecules* **2011**, *12*, 1387.
(5) Arnon, H.; Granit, R.; Porat, R.; Poverenov, E. *Food Chem.* **2015**, *166*, 465.

DOI: 10.1021/jacs.6b10624
J. Am. Chem. Soc. 2017, 139, 803−810

(6) Quirós-Sauceda, A. E.; Ayala-Zavala, J. F.; Olivas, G. I.; González-Aguilar, G. A. *J. Food Sci. Technol.* **2014**, *51*, 1674.
(7) Calderón, M.; Quadir, M. A.; Sharma, S. K.; Haag, R. *Adv. Mater.* **2010**, *22*, 190.
(8) Ono, R. J.; Lee, A. L. Z.; Chin, W.; Goh, W. S.; Lee, A. Y. L.; Yang, Y. Y.; Hedrick, J. L. *ACS Macro Lett.* **2015**, *4*, 886.
(9) Reineke, T. M. *ACS Macro Lett.* **2016**, *5*, 14.
(10) Chacko, R. T.; Ventura, J.; Zhuang, J.; Thayumanavan, S. *Adv. Drug Delivery Rev.* **2012**, *64*, 836.
(11) Torchilin, V. P. *Adv. Drug Delivery Rev.* **2012**, *64*, 302.
(12) Kamaly, N.; Yameen, B.; Wu, J.; Farokhzad, O. C. *Chem. Rev.* **2016**, *116*, 2602.
(13) de la Rica, R.; Aili, D.; Stevens, M. M. *Adv. Drug Delivery Rev.* **2012**, *64*, 967.
(14) Amir, R. J.; Zhong, S.; Pochan, D. J.; Hawker, C. J. *J. Am. Chem. Soc.* **2009**, *131*, 13949.
(15) Samarajeewa, S.; Shrestha, R.; Li, Y.; Wooley, K. L. *J. Am. Chem. Soc.* **2012**, *134*, 1235.
(16) Guo, D. S.; Wang, K.; Wang, Y. X.; Liu, Y. *J. Am. Chem. Soc.* **2012**, *134*, 10244.
(17) Samarajeewa, S.; Zentay, R. P.; Jhurry, N. D.; Li, A.; Seetho, K.; Zou, J.; Wooley, K. L. *Chem. Commun. (Cambridge, U. K.)* **2014**, *50*, 968.
(18) Kashyap, S.; Singh, N.; Surnar, B.; Jayakannan, M. *Biomacromolecules* **2016**, *17*, 384.
(19) Kühnle, H.; Börner, H. G. *Angew. Chem., Int. Ed.* **2009**, *48*, 6431.
(20) Guo, J.; Zhuang, J.; Wang, F.; Raghupathi, K. R.; Thayumanavan, S. *J. Am. Chem. Soc.* **2014**, *136*, 2220.
(21) Azagarsamy, M. A.; Sokkalingam, P.; Thayumanavan, S. *J. Am. Chem. Soc.* **2009**, *131*, 14184−14185.
(22) Wang, H.; Raghupathi, K. R.; Zhuang, J.; Thayumanavan, S. *ACS Macro Lett.* **2015**, *4*, 422.
(23) Trappmann, B.; Ludwig, K.; Radowski, M. R.; Shukla, A.; Mohr, A.; Rehage, H.; Böttcher, C.; Haag, R. *J. Am. Chem. Soc.* **2010**, *132*, 11119.
(24) Burakowska, E.; Zimmerman, S. C.; Haag, R. *Small* **2009**, *5*, 2199.
(25) Whitton, G.; Gillies, E. R. *J. Polym. Sci., Part A: Polym. Chem.* **2015**, *53*, 148.
(26) Hu, J.; Zhang, G.; Liu, S. *Chem. Soc. Rev.* **2012**, *41*, 5933.
(27) Ghadiali, J. E.; Stevens, M. M. *Adv. Mater.* **2008**, *20*, 4359.
(28) Zelzer, M.; Todd, S. J.; Hirst, A. R.; McDonald, T. O.; Ulijn, R. V. *Biomater. Sci.* **2013**, *1*, 11.
(29) Raghupathi, K. R.; Azagarsamy, M. a.; Thayumanavan, S. *Chem. - Eur. J.* **2011**, *17*, 11752.
(30) Habraken, G. J. M.; Peeters, M.; Thornton, P. D.; Koning, C. E.; Heise, A. *Biomacromolecules* **2011**, *12*, 3761.
(31) Figg, C. A.; Kubo, T.; Sumerlin, B. S. *ACS Macro Lett.* **2015**, *4*, 1114.
(32) Tucker, B. S.; Getchell, S. G.; Hill, M. R.; Sumerlin, B. S. *Polym. Chem.* **2015**, *6*, 4258.
(33) Harnoy, A. J.; Rosenbaum, I.; Tirosh, E.; Ebenstein, Y.; Shaharabani, R.; Beck, R.; Amir, R. J. *J. Am. Chem. Soc.* **2014**, *136*, 7531.
(34) Rosenbaum, I.; Harnoy, A. J.; Tirosh, E.; Buzhor, M.; Segal, M.; Frid, L.; Shaharabani, R.; Avinery, R.; Beck, R.; Amir, R. J. *J. Am. Chem. Soc.* **2015**, *137*, 2276.
(35) Harnoy, A. J.; Slor, G.; Tirosh, E.; Amir, R. J. *Org. Biomol. Chem.* **2016**, *14*, 5813.
(36) Gitsov, I.; Wooley, K. L.; Hawker, C. J.; Ivanova, P. T.; Fréchet, J. M. J. *Macromolecules* **1993**, *26*, 5621.
(37) Gitsov, I.; Wooley, K. L.; Fréchet, J. M. J. *Angew. Chem., Int. Ed. Engl.* **1992**, *31*, 1200.
(38) Hoogenboom, R. *Angew. Chem., Int. Ed.* **2010**, *49*, 3415.
(39) Albertazzi, L.; Mickler, F. M. F. M.; Pavan, G. M. G. M.; Salomone, F.; Bardi, G.; Panniello, M.; Amir, E.; Kang, T.; Killops, K. L. K. L.; Bräuchle, C.; Amir, R. J. R. J.; Hawker, C. J. C. J. *Biomacromolecules* **2012**, *13*, 4089.
(40) Neises, B.; Steglich, W. *Angew. Chem., Int. Ed. Engl.* **1978**, *17*, 522.
(41) Gillies, E. R.; Jonsson, T. B.; Fréchet, J. M. J. *J. Am. Chem. Soc.* **2004**, *126*, 11936.
(42) Buzhor, M.; Avram, L.; Frish, L.; Cohen, Y.; Amir, R. J. *J. Mater. Chem. B* **2016**, *4*, 3037.
(43) Kornreich, M.; Avinery, R.; Beck, R. *Curr. Opin. Biotechnol.* **2013**, *24*, 716−723.
(44) Amir, R. J. *Synlett* **2015**, *26*, 2617.
(45) Eppel, S.; Portnoy, M. *J. Phys. Chem. B* **2014**, *118*, 9733.

DOI: 10.1021/jacs.6b10624
J. Am. Chem. Soc. 2017, 139, 803−810